Prospects of a Meshed Electrical Distribution System Featuring Large-Scale Variable Renewable Power

Marco R. M. Cruz [1], Desta Z. Fitiwi [2], Sérgio F. Santos [1] [iD], Sílvio J. P. S. Mariano [3] [iD] and João P. S. Catalão [1,4,5,*]

1   C-MAST, University of Beira Interior, 6201-001 Covilhã, Portugal; marco.r.m.cruz@gmail.com (M.R.M.C.);
     sdfsantos@gmail.com (S.F.S.)
2   Energy and Environment Department, Economic and Social Research Institute, Dublin, Ireland;
     destinzed@gmail.com
3   Instituto de Telecomunicações and University of Beira Interior, 6201-001 Covilhã, Portugal; sm@ubi.pt
4   INESC TEC and the Faculty of Engineering, University of Porto, 4200-465 Porto, Portugal
5   INESC-ID, Instituto Superior Técnico, University of Lisbon, 1049-001 Lisbon, Portugal
*   Correspondence: catalao@fe.up.pt

Abstract: Electrical distribution system operators (DSOs) are facing an increasing number of challenges, largely as a result of the growing integration of distributed energy resources (DERs), such as photovoltaic (PV) and wind power. Amid global climate change and other energy-related concerns, the transformation of electrical distribution systems (EDSs) will most likely go ahead by modernizing distribution grids so that more DERs can be accommodated. Therefore, new operational strategies that aim to increase the flexibility of EDSs must be thought of and developed. This action is indispensable so that EDSs can seamlessly accommodate large amounts of intermittent renewable power. One plausible strategy that is worth considering is operating distribution systems in a meshed topology. The aim of this work is, therefore, related to the prospects of gradually adopting such a strategy. The analysis includes the additional level of flexibility that can be provided by operating distribution grids in a meshed manner, and the utilization level of variable renewable power. The distribution operational problem is formulated as a mixed integer linear programming approach in a stochastic framework. Numerical results reveal the multi-faceted benefits of operating distribution grids in a meshed manner. Such an operation scheme adds considerable flexibility to the system and leads to a more efficient utilization of variable renewable energy source (RES)-based distributed generation.

Keywords: electrical distribution systems; meshed topology; mixed integer linear programing; stochastic programming; variable renewable power; flexibility option

1. Introduction

1.1. Framework and Motivation

Distribution power systems are experiencing massive transformations that are buoyed by the increasing need to integrate more variable renewable-type distributed generations (DGs). This means that distribution grids will be equipped with the necessary tools to enable bidirectional power flows, which is contrary to their traditional setup [1–7]. Also, such a massive transformation needs to be accompanied by new operational schemes. In other words, new operational strategies should be crafted and widely used in order to increase the degree of flexibility in the distribution systems, and hence the penetration of renewables, such as photovoltaic (PV) and wind power. This is due to the

fact that the traditional radial network operation strategy may not be sufficient to accommodate the increasing penetration of renewables and for their efficient utilization.

In this context, smart grids are one of the most promising solutions that enable large-scale integration of variable renewable energy sources (vRESs) at a distribution level [8–12]. However, the scale of transformation that is required to "smartify" existing grids means that the whole process may be costly and, most importantly, slow. In other words, the smartification process will not happen overnight; it will, rather, involve a series of time-consuming and expensive upgrades to existing network infrastructures. Hence, the impact of smart grids would only be felt in the long-run when they have fully materialized.

Most of the traditional distribution networks are meshed by design, but they are operated radially only due to technical limitations that are mainly related to system protection. These limitations are discussed in [13]. This means that some tie-lines (also known as switches) are kept open so that the grid's topology remains radial. Thus far, it has been easier to operate and protect a radial topology [13–16].

The lines that are normally open in radial network systems are only used in emergency situations, e.g., situations of fault or power supply failure. The main purpose of this is to enhance the reliability of power delivery, i.e., some of the tie-lines that are normally open are closed to re-route power flows so that the amount of load that is shed is minimized. However, the radiality of the network system is maintained at all times, regardless of the operational situations that happen in the system. The good news is that, in well-planned distribution networks, contingencies or emergency situations are rare phenomena.

As previously mentioned, one strategy worth considering is the operation of distribution networks in a meshed topology. This type of topology is contrary to what is well-established; that is, radially operating distribution systems. However, with the technological advances that are now available, and expected to happen in the near future in an even more accelerated manner, it is possible to deal with all of the inherent limitations of the meshed operation of distribution networks. Given its multi-faceted benefits, the so-called meshed topology is expected to be a normal operation scheme for distribution grids in the future. However, this does not mean that a radial topology would be completely abolished; there may be cases where this would make more sense from an economic and a technical standpoint.

The advantages that meshed distribution systems have are the reduction of power losses, improved voltage profiles, more flexibility, the capability to deal with high electricity demand growth, and the enhancement of power quality (PQ) [17]. Furthermore, in meshed distribution systems with no integrated DGs, the distribution of power flows among parallel paths can potentially decrease the stress on the entire network system, and possibly defer grid-related investments. This can be achieved only by optimizing the loops in tie-lines in the distribution system. When DGs are appropriately allocated in such systems, they can bring about several benefits, such as a reduction of power losses, a better voltage profile, and also an investment deferral as a result of reduced congestion in the network components (feeders and transformers) [17].

Likewise, a meshed topology can provide similar benefits to those of DGs. The combination of both can potentially enhance distribution system reliability and the quality of the power that is delivered to end-users. The negative aspects that are associated with DG integration are the possible increase in short circuit currents and, hence, a possible need for modification of protection devices' settings [17].

Because of this, international standards determine the immediate disconnection of DGs from the distribution system in case of faults so that conventional protection devices can act properly. Similarly, a meshed topology also shares this issue. However, technological advances make it easier to switch from meshed to a radial topology in case of fault or vice versa, allowing us to reap the benefits of a meshed topology. For example, locally generated renewable power can be efficiently utilized under a meshed topology, which would otherwise have been curtailed in the traditional network setup.

There are a set of technologies that could be used to exploit a meshed network topology, and minimize the limitations of such a topology. For instance, when a fault occurs in the system, fast de-loopers can be deployed to quickly switch from a meshed to a radial topology so that conventional protection devices can properly act. Another enabling technology with regards to a meshed topology's operation is Fault Current Limits (FCLs) [18]. Generally, the operation of distribution networks in a meshed manner may become the norm in the near future.

1.2. Literature Review

The large-scale integration of vRESs has brought about a set of challenges that require attention and action. The main challenges involve protection schemes, voltage regulation as a result of fluctuations induced by vRESs, voltage sags and/or rises, and network congestion [19]. Such issues are exacerbated by the increasing integration of vRESs in distribution networks because these are designed for unidirectional power flows. However, operating distribution grids in a meshed manner can alleviate some of these issues, and bring about a number of benefits; for example, in terms accommodating more vRES power, which is an important aspect given the growing global concerns about climate change. However, the prospects of a meshed operational scheme have not been adequately explored in the literature.

A comparative study between a meshed operation and the reinforcement of distribution networks was conducted in [20]. The study involves the comparison of results from enumeration, constraints, and loops analysis methods. The authors in [21] develop a model that estimates the maximum penetration of DGs based on a steady state analysis. The approach uses some elements of an optimal power flow analysis and bus voltage and current flow limits to estimate the maximum allowable DG penetration at each node of the considered system. The authors conclude that a meshed topology may be a good alternative to host large-scale DG power. Furthermore, the authors in [22] propose a methodology for allocating conventional DGs in a distribution system, and evaluate their impacts on the distribution system. For the analysis, they have considered a meshed operational scheme and a voltage sensitivity index to quantify the operability of the system. However, their analysis is based on the integration of conventional sources of energy into distribution systems. In [23], the authors provide an extensive analysis of optimum power flows when operating distribution networks in a radial and a meshed manner. The analysis is carried out considering reactive power compensation devices and DGs. In [24], the authors develop an operational model for analyzing the prospects of a meshed distribution network topology, which is based on circuits composed of a resistor, inductor, and capacitor (RLC). Reference [25] provides a steady state analysis of a meshed distribution system featuring DGs, and is based on iterative load-flow calculations. However, the analysis of the existing literature, reviewed here, is based on conventional DGs under a meshed operational scheme. To the best of our knowledge, the topic of integrating vRESs in tandem with meshed operation of distribution systems has not been addressed in the literature. Hence, this is the main focus of the current work. The argument provided here is that electrical distribution systems can be operated in a meshed topology under normal situations. Additionally, they can be equipped with advanced, and even currently available, technologies that temporarily enable a smooth automated transition to a radial topology in case of a contingency, and back to the preferred topology when the fault is cleared. This way, one can take full advantage of the meshed operation of the distribution network, which eventually leads to reduced losses, improved voltage profiles, and a more efficient management of locally produced vRES power. The meshed operational scheme can also have benefits in terms of network-related investments. The more distributed nature of power flows in the meshed topology would mean lower stress (congestion) in the whole system, reducing the need for network upgrades. Note that existing switches and loops in distribution systems can be effectively used to develop an optimal meshed topology.

1.3. Contributions and the Paper's Organization

The increasing penetration of vRESs into distribution networks unfortunately leads to some technical challenges. Appropriate tools and methods need to be developed and deployed to address these challenges. One example is exploring different operating strategies, which forms the core analysis of the subject matter that is contained in our current work. The main enabling mechanisms of a meshed operational scheme in a distribution network are discussed.

An appropriate mathematical formulation is developed to support our analysis. The formulation is an operational model that is based on a least-cost optimization formulated under a stochastic programming framework to account for the uncertainty that arises from various sources, such as renewable power production and electricity demand. The analysis encompasses an optimal network topology, losses, voltage profiles, costs, and other operational variables of the considered distribution network. The resulting model is of a stochastic mixed integer linear programming type, whose objective function is minimized to achieve the optimal operation of a system that features large quantities of vRES power, while respecting a number of technical, economic, and environmental constraints. An extensive analysis is performed with respect to the flexibility that a meshed topology can provide, and the impact on the integration and utilization levels of vRESs.

This work is organized as follows. The mathematical model used in this work is described in Section 2. Section 3 presents details of the case studies that are considered in this work, and discusses the numerical results that were obtained. Section 4 provides concluding remarks and further insights.

2. Mathematical Model

In this section, we provide a broad description of the developed stochastic optimization model, which is of a mixed integer linear programming nature. The model is used to conduct an analysis of the optimal operation of meshed distribution systems with large-scale renewable integration. The meshed operation is analyzed in terms of the use level of locally produced vRES power without adversely affecting the operation of the system. A linearized alternating current (AC) power flow model is used. This model guarantees a correct balance between accuracy and computational requirements. Note that the acronyms used in the mathematical formulation are presented in Appendix A.

2.1. Objective Function

The main objective is to minimize the total costs of operating the considered distribution system. These costs are associated with the operating costs in the system, namely the cost of energy not supplied, the costs of emissions, and the cost of power generation using conventional and renewable power sources.

$$Minimize\ TOC = TEC + TENSC + TEmiC \tag{1}$$

Equation (1) minimizes the *TOC*, which represents the total expected cost in the system.

The first term in (1) represents the expected costs of producing energy using renewable technologies (solar and wind in this case), and purchasing energy from the upstream network as in (2). The two terms in (2) are calculated by (3) and (4), respectively.

$$TEC = EC^{vRES} + EC^{SS} \tag{2}$$

$$EC^{vRES} = \sum_{s \in \Omega^s} \rho_s \sum_{h \in \Omega^h} \sum_{g \in \Omega^g} OC_g P_{g,i,s,h}^{vRES}, \tag{3}$$

$$EC^{SS} = \sum_{s \in \Omega^s} \rho_s \sum_{h \in \Omega^h} \sum_{\varsigma \in \Omega^\varsigma} \lambda_h^\varsigma P_{c,s,h}^{SS}. \tag{4}$$

Regarding the second term of (1), TENSC represents the cost of energy not supplied. This term is based on the calculation of the active and reactive power that was not supplied, and is given by Equation (5).

$$TENSC = \sum_{s\in\Omega^s} \rho_s \sum_{h\in\Omega^h} \sum_{i\in\Omega^i} \left(v_{s,h}^P P_{i,s,h}^{NS} + v_{s,h}^Q Q_{i,s,h}^{NS} \right) \tag{5}$$

The terms $v_{s,h}^P$ and $v_{s,h}^Q$ are defined as penalty factors. They correspond to penalty terms that are associated with any active and reactive power that is shed. These must be set to sufficiently high values to avoid unnecessary load shedding. Finally, the term $TEmiC^{vRES}$ represents the expected cost of emissions. These emissions are related to energy production from renewable sources, as well as conventional ones, and that of energy purchased from the upstream network. This term is defined by:

$$TEmiC = TEmiC^{vRES} + EmiC^{SS}. \tag{6}$$

The corresponding terms in (5) are expressed by:

$$TEmiC^{vRES} = \sum_{s\in\Omega^s} \rho_s \sum_{h\in\Omega^h} \sum_{g\in\Omega^g} \sum_{i\in\Omega^i} \lambda^{CO_2} ER_g^{vRES} P_{g,i,s,h}^{vRES}, \tag{7}$$

$$EmiC^{SS} = \sum_{s\in\Omega^s} \rho_s \sum_{h\in\Omega^h} \sum_{\varsigma\in\Omega^\varsigma} \sum_{i\in\Omega^i} \lambda^{CO_2} ER_\varsigma^{SS} P_{\varsigma,s,h}^{SS}. \tag{8}$$

2.2. Constraints

Kirchhoff's current law must be enforced for active (9) and reactive (10) power flows. These ensure that the sum of incoming flows must be equal to the outgoing ones. These conditions must be respected at all times for safe operation of the system.

$$\sum_{g\in\Omega^g} P_{g,i,s,h}^{vRES} + P_{\varsigma,s,h}^{SS} + P_{i,s,h}^{NS} + \sum_{in,k\in\Omega^k} P_{k,s,h} - \sum_{out,k\in\Omega^k} P_{k,s,h} = PD_{s,h}^i +$$
$$\sum_{in,k\in\Omega^k} \tfrac{1}{2} PL_{k,s,h} + \sum_{out,k\in\Omega^k} \tfrac{1}{2} PL_{k,s,h}; \forall \varsigma\epsilon\Omega^\varsigma; \forall \varsigma\epsilon i; k\epsilon i, \tag{9}$$

$$\sum_{g\in\Omega^g} Q_{g,i,s,h}^{vRES} + Q_{\varsigma,s,h}^{SS} + Q_{i,s,h}^{NS} + \sum_{in,k\in\Omega^k} Q_{k,s,h} - \sum_{out,k\in\Omega^k} Q_{k,s,h} = QD_{s,h}^i +$$
$$\sum_{in,k\in\Omega^k} \tfrac{1}{2} QL_{k,s,h} + \sum_{out,k\in\Omega^k} \tfrac{1}{2} QL_{k,s,h}; \forall \varsigma\epsilon\Omega^\varsigma; \forall \varsigma\epsilon i; k\epsilon i. \tag{10}$$

On the left-hand side of Equation (9), we can see that the active power flows from the renewable power generation as well as the power that is injected at the substation. On the other side of the equation, we have the power flow that is associated with the demand and the losses (treated here as fictitious loads). The same principles apply to the reactive power flow shown in (10).

Kirchhoff's voltage law must also be considered. This restriction governs the power flow in the feeders, which are represented by linearized power flow equations considering two practical assumptions. The first one states that the voltage magnitude is essentially close to the nominal value V_{nom}. The second one is related to the difference of voltage angles θ_k. For security systems, this difference has to be as small as possible, which leads to a trigonometric approximation $\sin\theta_k \approx \theta_k$ and $\cos\theta_k \approx 1$. Considering these two simplifying assumptions, the active and reactive AC power flow equations can be linearized, and represented as in:

$$\left| P_{k,s,h} - \left(V_{nom}\left(\Delta V_{i,s,h} - \Delta V_{j,s,h} \right) g_k - V_{nom}^2 b_k \theta_{k,s,h} \right) \right| \le MP_k(1 - u_{k,h}), \tag{11}$$

$$\left| Q_{k,s,h} - \left(- V_{nom}\left(\Delta V_{i,s,h} - \Delta V_{j,s,h} \right) b_k - V_{nom}^2 g_k \theta_{k,s,h} \right) \right| \le MQ_k(1 - u_{k,h}), \tag{12}$$

$$\text{where } \Delta V^{min} \le \Delta V_{i,s,h} \le \Delta V^{max}. \tag{13}$$

In relation to the power flows in each branch, these cannot exceed the maximum transfer capacity:

$$P_{k,s,h}^2 + Q_{k,s,h}^2 \leq u_{k,h}(S_k^{max})^2. \tag{14}$$

The active and reactive power losses in each branch are algebraically represented by:

$$PL_{k,s,h} = R_k\left(P_{k,s,h}^2 + Q_{k,s,h}^2\right)/V_{nom}^2, \tag{15}$$

$$QL_{k,s,h} = X_k\left(P_{k,s,h}^2 + Q_{k,s,h}^2\right)/V_{nom}^2. \tag{16}$$

Note that Equations (14)–(16) are easily linearized using a piecewise linearization approach, which is common in the literature. Further explanation of the piecewise linearization can be found in Appendix B.

The active and reactive power limits of conventional as well as vRESs are also considered as constraints. Such constraints related to vRESs are given by (17) and (18):

$$P_{g,i,s,h}^{vRES,min} \leq P_{g,i,s,h}^{vRES} \leq P_{g,i,s,h}^{vRES,max}, \tag{17}$$

$$-\tan\left(\cos^{-1}\left(pf_g\right)\right)P_{g,i,s,h}^{vRES} \leq Q_{g,i,s,h}^{vRES} \leq \tan\left(\cos^{-1}\left(pf_g\right)\right)P_{g,i,s,h}^{vRES}. \tag{18}$$

where pf_g is the power factor of generator g.

The reactive power injected or withdrawn at a substation in the system is subject to a minimum and a maximum level as in (18). This is motivated by security concerns.

$$-\tan\left(\cos^{-1}(pf_{ss})\right)P_{\varsigma,s,h}^{SS} \leq Q_{\varsigma,s,h}^{SS} \leq \tan\left(\cos^{-1}(pf_{ss})\right)P_{\varsigma,s,h}^{SS}, \tag{19}$$

Note that the voltage angle difference $\theta_{k,s,h}$ is defined as $\theta_{k,s,h} = \theta_{i,s,h} - \theta_{j,s,h}$. In this case, i and j belong to the same branch k.

3. Results

3.1. Data and Assumptions

In this work, we use a standard 119-bus distribution system to perform the required analysis. The schematic diagram of this system is shown in Figure 1. The main data of the considered system are summarized in Table 1. Further information about the test system and data can be found in [3]. The size and location of vRESs are adapted from [3], as can be seen in Table 2. More of the data-related assumptions that were made in this analysis are presented in Tables 3–5. Further assumptions are summarized as follows:

- The operational analysis is based on a 24-h period, subdivided on an hourly basis.
- The maximum voltage deviation at each bus is set to $\pm 5\%$ of the nominal value (which, in this case, is 11 kV).
- In all simulations, the substation is treated as the reference node, in which both the voltage deviation and the angle are set to zero.
- The number of partitions considered for linearizing quadratic terms is 5, which is in line with the findings in [26].
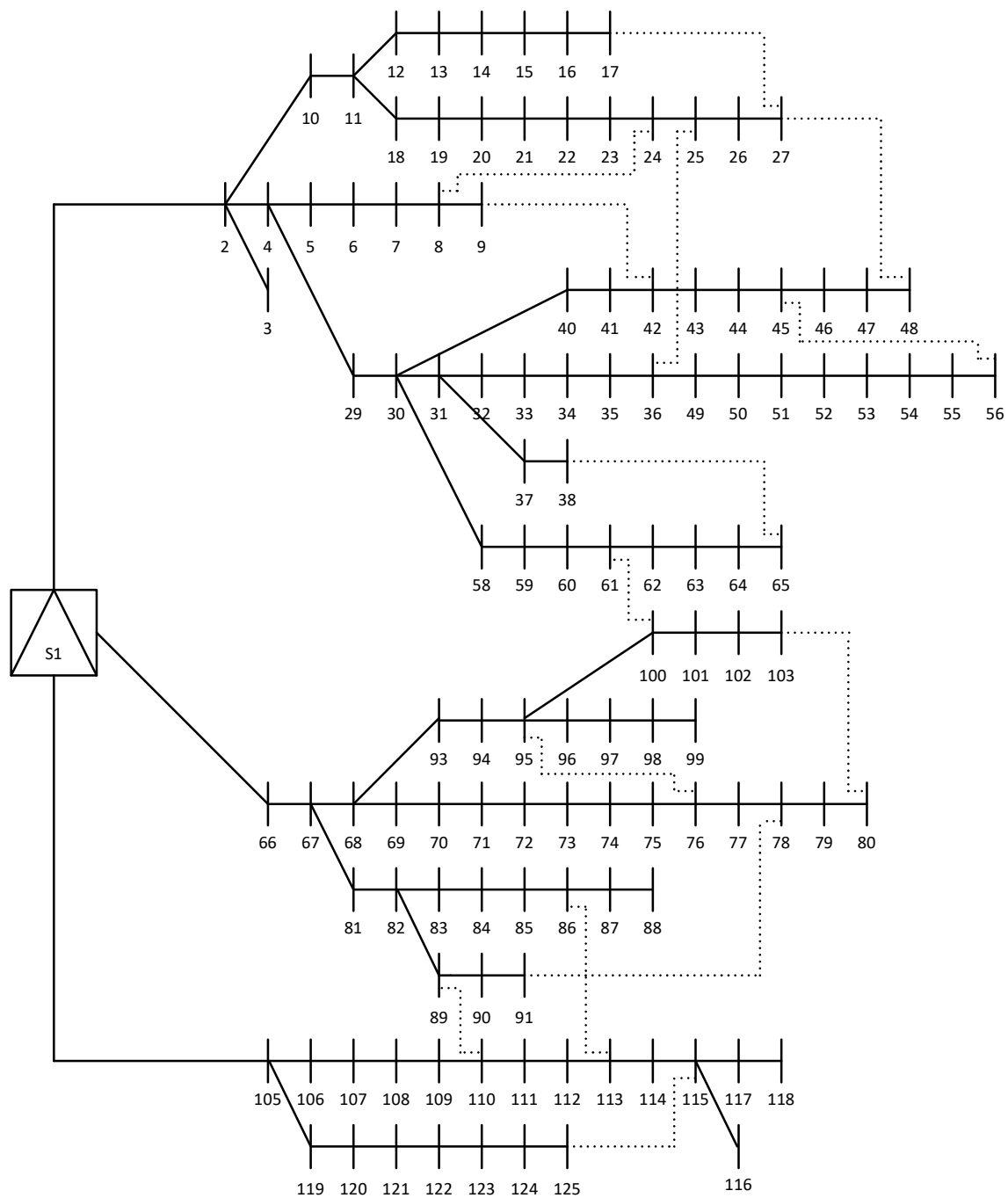
Figure 1. A schematic diagram of the 119-bus test system.

Table 1. General system data.

Parameter Description	Parameter Setting
Nominal voltage	11 kV
Active power demand	22,709.720 kW
Reactive power demand	17,041.068 kVAr
Base case system losses	1298.090 kW
Minimum voltage of the base case system (which occurs at bus 116)	0.8783 p.u.

Table 2. The size and location of wind- and photovoltaic (PV)-type distributed generations (DGs).

Bus	Wind (MW)	PV (MW)
14	1	0
21	1	0
24	1	0
25	0	1
29	0	1
32	1	0
33	1	0
35	0	1
37	1	0
38	1	0
42	1	0
43	0	1
44	1	1
52	1	1
53	1	0
56	1	0
61	1	0
69	1	0
73	1	1
74	1	0
77	1	1
79	0	1
82	1	0
83	1	0
84	0	1
85	1	0
89	1	0
96	1	0
100	1	1
101	0	1
106	0	1
108	1	0
112	1	1
114	1	1
116	1	1
117	0	1
119	0	1
121	1	0

Table 3. Further data-related assumptions.

Parameter	Setting
pf^{ss}	0.8
pf^{vRES}	0.95
ER^{ss}	0.4 tCO$_2$e/MWh
λ^{CO_2}	15 /tCO$_2$e
$v_{s,h}^{P}$	3000 /MW
$v_{s,h}^{Q}$	3000 /MVAr
MP_k, MQ_k	20

Table 4. The cost of electricity generation from renewable sources and emission rates.

DG Type	Variable Cost (€/MWh)	Emission Rates of DGs (tCO$_2$e/MWh)
Solar	40	0.0584
Wind	20	0.0276

Table 5. The maximum transfer capacity in feeders.

Feeders	Maximum Transfer Capacity (A)
{(1, 2); (2, 4); (1, 66); (66, 67)}	1200
{(4, 5); (5, 6); (6, 7); (4, 29); (29, 30); (30, 31); (67, 68); (67, 81); (81, 82); (1, 105); (105, 106); (106, 107)}	800
Remaining feeders	400

Our work involves power productions using variable renewable sources, such as wind and solar. The power outputs from these resources are subject to high-level uncertainty and variability. Demand is also variable (say throughout the course of the day), even if it can be fairly predicted more accurately than a variable renewable power output. The stochastic nature of our work arises as a result of these issues. Therefore, we have handled such stochastic parameters via a stochastic programming framework that accounts for the most plausible states of these parameters at a given future time, each of which is associated with a probability. Over the considered operational period (which in our case is 24-h long), such states collectively form scenarios, which are jointly considered in the optimization process.

In other words, the stochastic nature of RES power outputs and demand is accounted for by considering an adequate number of scenarios for each. Therefore, the power production profiles of wind- and solar-type DGs, as well as the demand profile, are assumed to be uniform throughout the system. The uncertainty associated with solar and wind power generations are taken into account by considering three different scenarios for each uncertain parameter. Demand uncertainty is also taken into account by considering six different scenarios each for residential- and industrial-type consumers. It should be noted that each scenario represents an hourly profile. The combination of these individual scenarios (which, in this case, is 81) results in the creation of the final set of scenarios that is used in our studies.

3.2. Numerical Results

As stated above, the analysis is carried out to study the operational flexibility that can be provided by operating vRES-rich distribution grids in a meshed manner. In addition, the analysis includes the impact of such a scheme on the use and integration of vRESs.

A total of six case studies are considered, designated as Case A to Case F. Case A is the Base Case, which neither considers network reconfiguration nor meshed operation. In Case B, network reconfiguration is allowed but always while maintaining a radial topology. Cases C to F all consider a meshed operational scheme, but with different levels of meshing (30% in Case C, 60% in case D, 80% in Case E, and 100% in Case F). The network configurations for the last four cases are presented in Figure 2. Note that meshing the distribution network makes use of existing tie-lines. For Cases B to F, the upper and lower voltage boundaries have been enforced. Table 6 shows the total expected cost, along with a breakdown of this cost and the total expected power losses in the system.

Table 6. The total expected costs of the objective function and power losses. PNS: Power Not Served.

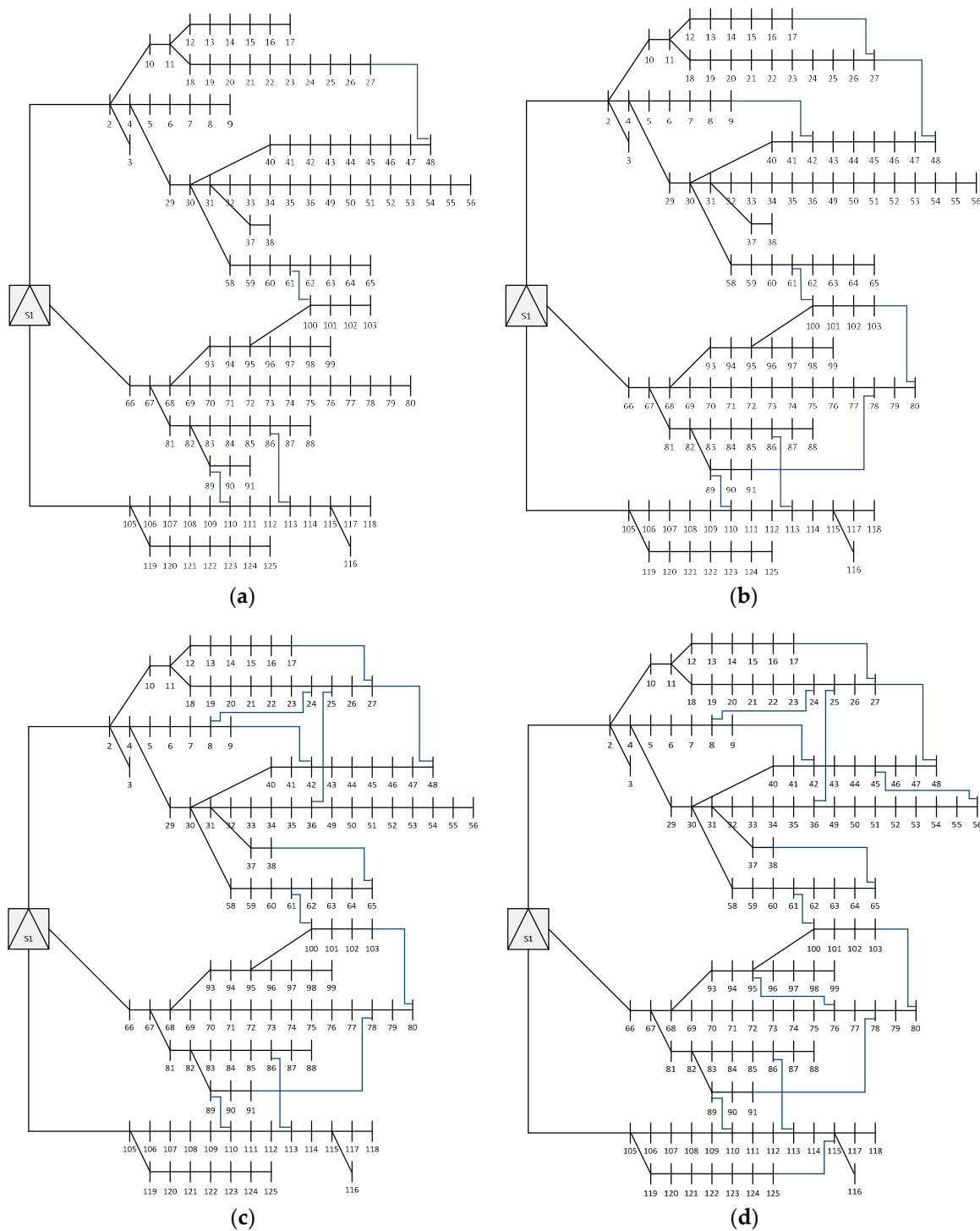|	Case A	Case B	Case C	Case D	Case E	Case F
Total Cost (€)	32,217.38	27,215.55	24,634.12	18,458.99	16,937.63	15,664.99
Energy Cost (€)	30,349.82	26,629.07	24,103.04	17,979.25	16,501.48	15,265.23
Emission Cost (€)	1219.56	557.47	513.63	472.96	436.15	399.76
PNS Cost (€)	647.99	29.01	17.45	6.78	0.00	0.00
Power Loss (MW)	20.25	9.39	8.01	7.21	6.47	5.73
Power Loss (MVar)	14.11	6.13	4.67	3.97	3.24	2.49

Figure 2. A schematic diagram of the meshed systems associated with Case C to Case F. (**a**) The 30% meshed network topology for Case C; (**b**) the 60% meshed network topology for Case D; (**c**) the 80% meshed network topology for Case E; and (**d**) the 100% meshed network topology for Case F.

Among the considered cases, the Base Case has the highest value of total costs, as expected. This is because all of the energy required in the system is imported through the substation. The energy mix associated with the Base Case can be seen in Figure 3a. Apart from the costs, the power losses in the system are also the highest among those computed in the remaining cases.
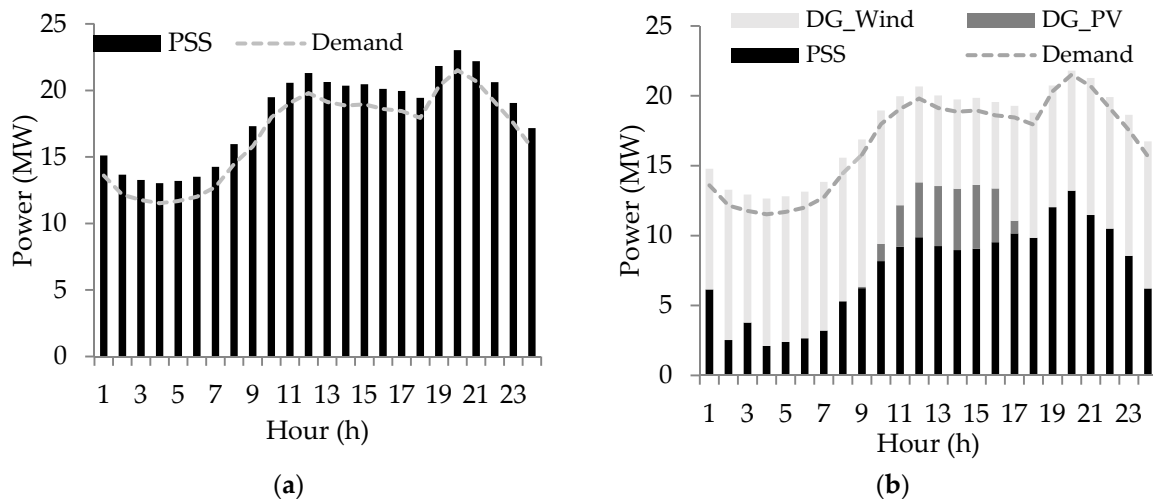
Figure 3. Energy mixes in the (**a**) Base Case and (**b**) Case B. PSS: Power from Substation; DG: distributed generation.

In Case B, the expected energy costs are reduced by 12%, the expected emissions costs by 54%, and the expected Power Not Served (PNS) costs by 96%. Overall, this translates into a reduction of 16% in expected total cost in the system. The decreases registered in the expected energy and emission costs are mainly due to the locally produced vRES power that is cheaper and "cleaner". The active and reactive power losses in the system are reduced on average by 54% and 70%, respectively. This is as a result of the combined effect of the DG integration and the optimal network reconfiguration. Most of the demand is met by locally generated power, which does not require heavy utilizations of existing feeders, and hence results in reduced losses. It has been proven that an optimal reconfiguration also reduces losses in the system. Figure 3b shows Case B's energy mix. In this figure, it can be seen that this case has 60.4% of the demand met by vRES power (of which 6.6% comes from solar-type and 53.9% from wind-type DGs).

Cases C through F are the ones that represent a system that is operated in a meshed network topology, but with increasing levels of "meshedness". In Case C, a 24% greater reduction in the expected total cost is observed, as a result of reductions in the individual cost terms (energy, emission, and PNS costs), in comparison with that of the Base Case. Active and reactive power losses also see reductions on average by 60% and 77%, respectively. With the increase in the "meshedness" level of the network, the reductions become more pronounced. In Case C, the percentage of demand covered by vRES power is 69.7% (of which 7.3% comes from solar and 62.4% from wind). In comparison to the radial topology in the Base Case, even the less-meshed topology sees further improvement in the utilization level of vRES power production. A further observation is the fact that even a weakly meshed distribution network (with a 30% connectedness index) shows an improvement of 9.3% in terms of vRES power generation compared to that of an optimally reconfigured radial topology.

In Cases D and E, where the "meshedness" levels are 60% and 80%, respectively, one can observe 43% and 47% overall cost reductions, respectively. In comparison to that of the Base Case, these can be regarded as significant improvements, and these generally show the favorable impact of meshed system operation. In Case E, the PNS costs are reduced by 100%. This can be explained by the fact that meshing the grid routes vRES power to where it is consumed. This would otherwise be shed in the radial (or weakly meshed) topology. As a result, the share of renewables in the total consumption in the above two cases (i.e., Cases D and E) amounts to 73.6% and 75.1%, respectively.

The last case—Case F—(where all branches are connected, creating a completely meshed network) yields the best operational results among the considered cases. Compared to the Base Case, a 51% reduction in overall cost can be seen. In terms of individual cost terms, the reductions are 50% in expected energy costs, 67% in emission costs, and 100% in expected PNS costs. System-wide average

losses are slashed down by 72% (active) and 88% (reactive). Regarding the energy mix, the fully meshed network, i.e., Case F, has a total of 75.8% of the total energy demand met by vRES energy (out of which 10.7% comes from solar-type and 65.1% from wind-type DGs). From Case A to Case F, one can easily notice the reductions in terms of energy imported from upstream (see in Table 6). In Case F, the entire system operates in near island mode (see hours 4 and 5, in which only 3% of demand in these hours is covered by importing power from the upstream network). Also, numerical results highlight that a fully meshed topology increases the utilization level of vRESs power generation by 15.4% compared to that of an optimally reconfigured radial topology. This translates into an approximately 42% decrease in the overall system cost, and 44% and 99% reductions in terms of expected energy and emission costs, respectively, as compared to that of a reconfigured radial topology, which is significant. The share of renewable power in the final energy consumption is as high as 75.8% in the case that incorporates a strongly meshed network, which is again noteworthy.

Figure 4a–d shows the energy mixes corresponding to the meshed cases, from low to a more complex meshed topology, respectively. The results in these figures reveal interesting variations in the utilization levels of vRES power productions during the 24-h period. It is also possible to see a decrease in the energy purchased from the upstream network (PSS) throughout the various case studies.
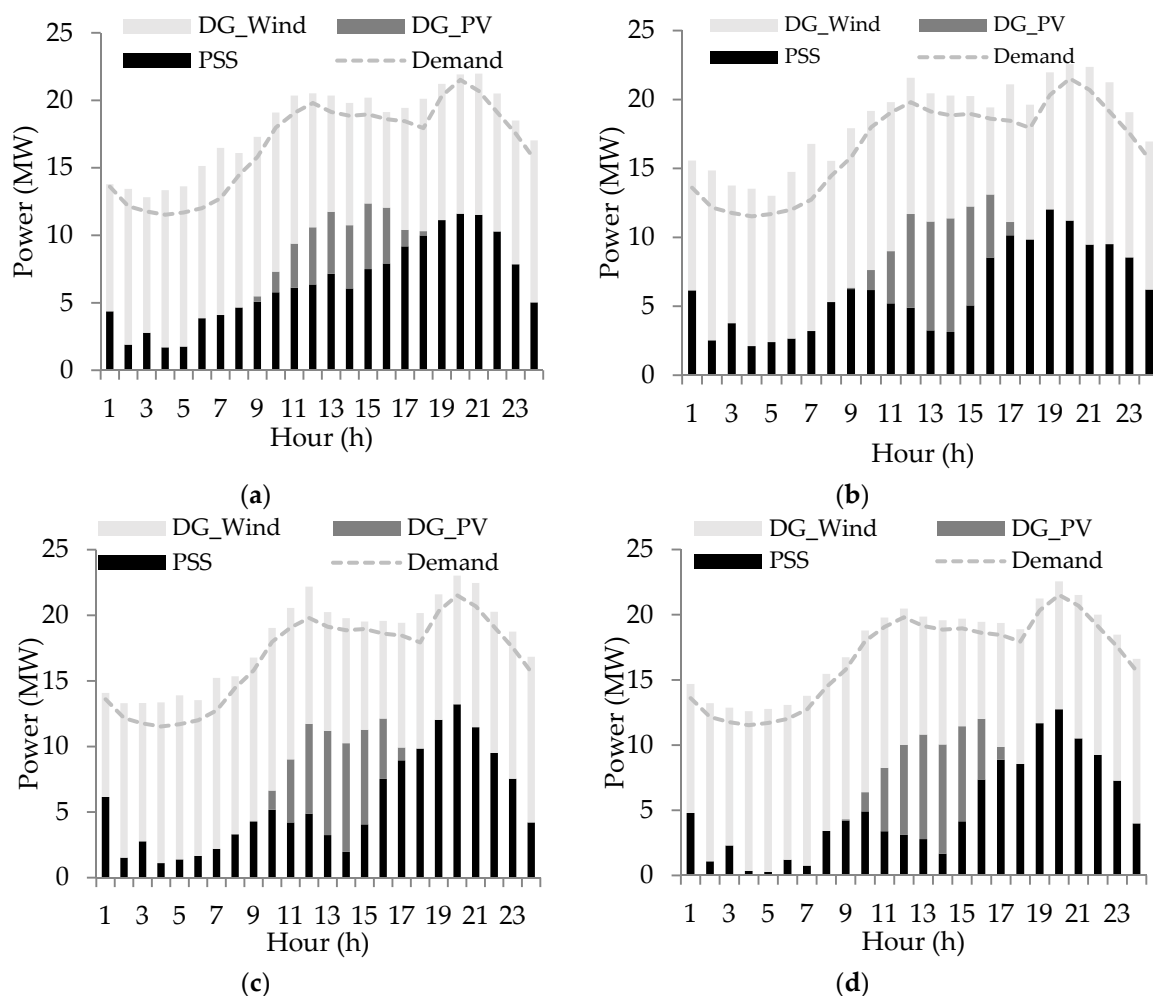

Figure 4. Energy mixes for different case studies. (**a**) Case C energy mix (30% meshed network); (**b**) Case D energy mix (60% meshed network); (**c**) Case E energy mix (80% meshed network); and (**d**) Case F energy mix (100% meshed network).

With regard to energy losses, the average profile of active power losses during the considered 24-h period of each case is shown in Figure 5. The results are in accordance with Table 6, dropping

from Case B to Case F, as has already been mentioned before. In Cases C to F, losses decrease within an interval, since, in addition to the DGs being near the loads, there are also now in some sections of the network smaller paths to be "traveled", resulting in a losses decrease.
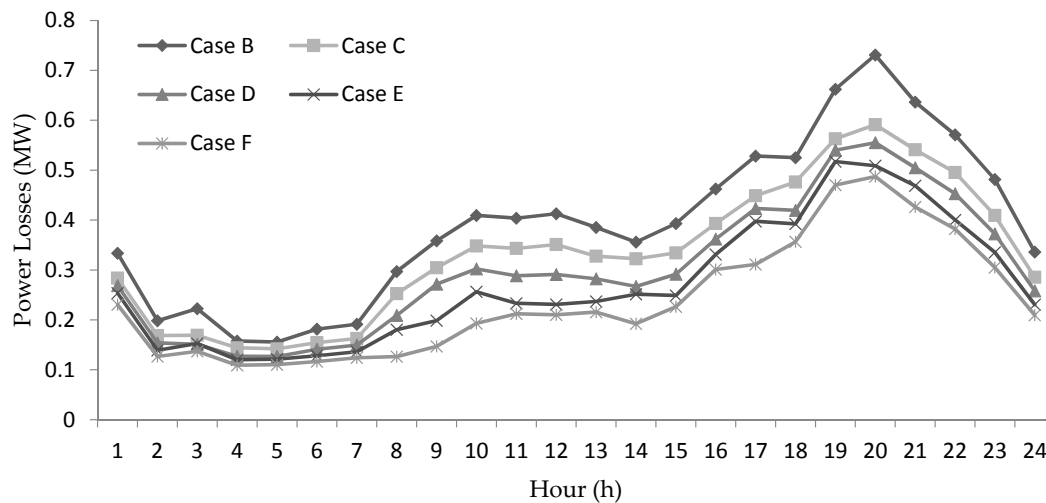

Figure 5. The power losses in the network associated with each case.

Figure 6 shows the average voltage profile corresponding to each case. The voltage deviation profile in Case A is the only one in which the deviations in some nodes surpasses the lower bound. In the remaining cases, where DGs are already integrated, all voltage deviations are significantly improved, and largely remain within the permissible range. In Case B as well as in the cases that involve network meshing (i.e., Cases C through F), voltage deviations do not show significant differences. In the figure, detailed voltage deviations for the nodes from 41 to 53 can be seen in the section that is zoomed out. In this particular section, we can see minor improvements in the voltage deviation, especially from Cases C through F. Generally, the case that has the most meshed network (i.e., Case F) has the best voltage deviation portfolio among the cases.
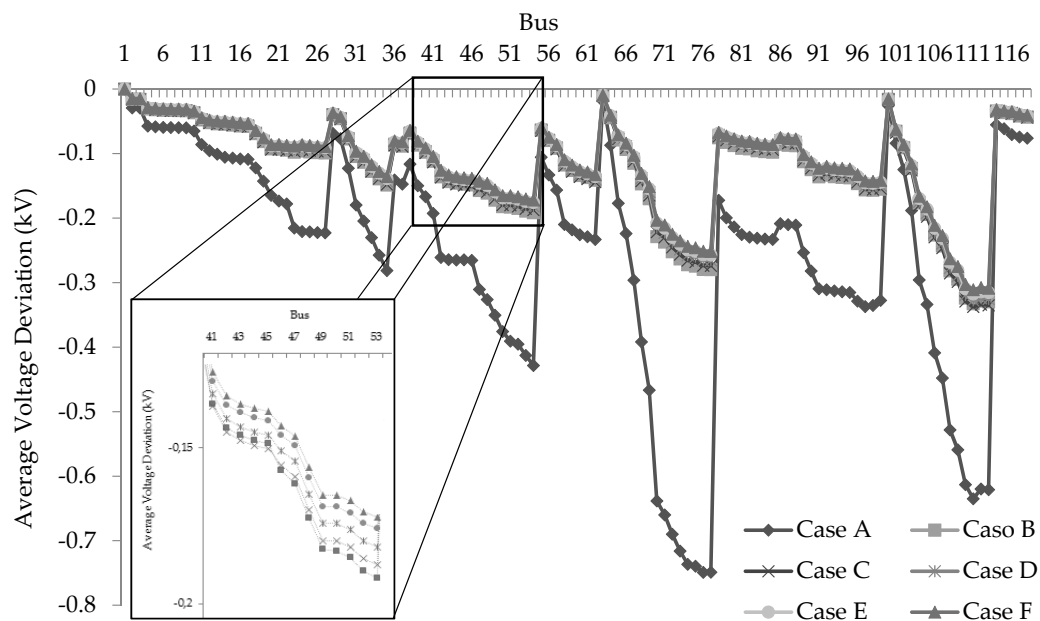

Figure 6. The average voltage deviation in all cases.

Total solar and wind power productions by node are shown in Figure 7a,b, respectively. In these figures, it is possible to observe the increased vRES power generation as one moves from Case B to Case F at each node. From the results in these figures, along with those in Figure 2, we can see the complementarity of meshed operation and renewable integration, in which a higher network meshing leads to a higher network flexibility and, hence, a greater increase in renewable integration.
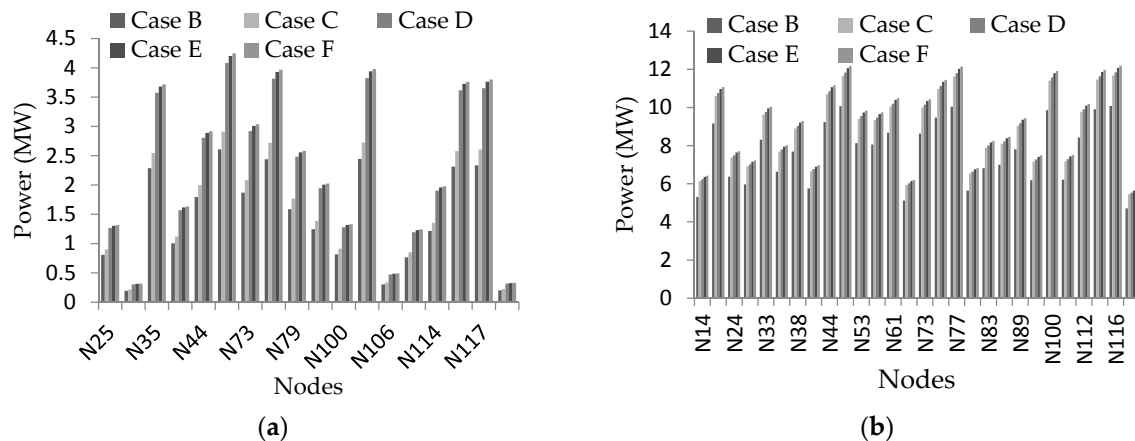

Figure 7. Variable renewable energy sources (vRES) outputs by node. (**a**) Solar power outputs by node (**b**) Wind power outputs by node.

Largely, the results obtained in the case studies, but especially in Case F, point out the immense contributions of the meshed operational scheme in terms of increasing system flexibility and the efficient utilization of vRESs in the system.

4. Conclusions

The work in this paper has explored the prospects of operating distribution network systems in a meshed topology, as opposed to the conventionally known radial operation. Furthermore, the contributions of a meshed network topology are studied in terms of enhancing system flexibility and its potential to increase the integration and efficient utilization of vRES power generation. To accomplish this, a stochastic mixed integer linear programming (SMILP) optimization model has been developed with a reasonably large scale distribution network as a test system. A linearized AC power flow is used, and the operational problem is formulated as a least-cost optimization while satisfying a number of technical, economic, and environmental constraints. Numerical results from the cases considered show that adopting a meshed network topology as a mainstream operational strategy for distribution systems has considerable benefits. Generally, a more meshed network leads to a better utilization of locally produced vRES power, and, hence, a higher share of renewable power. Even a weakly meshed distribution network (i.e., the case with a 30% connectedness index) results in a 9.3% increase in vRES power absorbed by the system during the considered time period. For the fully meshed topology case, the increase in the utilization level of vRES power amounts to 15.4% compared to that of an optimally reconfigured radial topology. This translates into a 42% decrease in the overall system cost. Also, the share of renewable power in the final energy consumption is as high as 75.8% in the case that incorporates a strongly meshed network, which is again noteworthy. Most importantly, all these improvements come without creating any undesirable effect on the operation of the considered distribution system. Instead, the average voltage profile is further enhanced, and the average power losses are significantly lowered. The results generally reveal the multi-faceted contributions and viability of a meshed operational strategy. It has been verified that this strategy adds valuable flexibility to distribution systems that are rich in vRES-based distribution generations. Such added system flexibility is an important asset to have for ensuring a more efficient utilization of variable renewable power generation in the system.

The authors will explore further opportunities for meshed operational schemes in the near future. In parallel to this, they intend to concentrate their focus on a detailed analysis in terms of its challenges when it comes to its practical implementation and propose possible solutions.

Author Contributions: Conceptualization, M.R.M.C., D.Z.F. and S.F.S.; Methodology, M.R.M.C., D.Z.F. and S.F.S.; Validation, D.Z.F. and J.P.S.C.; Writing, M.R.M.C., D.Z.F. and S.F.S.; Supervision, D.Z.F., S.J.P.S.M. and J.P.S.C.

Conflicts of Interest: The authors declare no conflict of interest.

Appendix A

The nomenclature that corresponds to the mathematical formulation that is presented in Section 2 can be seen in Table A1.

Table A1. Nomenclature.

Sets/Indices	Definitions	Sets/Indices	Definitions
i/Ω^i	Index/set of buses	$hh,h/\Omega^h$	Index/set of hourly snapshots
$g/\Omega^g/\Omega^{DG}$	Index/set of generators/vRES	s/Ω^s	Index/set of scenarios
k/Ω^k	Index/set of branches	$\varsigma/\Omega^\varsigma$	Index/set of substations
Parameters	Definitions	**Parameters**	Definitions
ER_g, ER_ς^{SS}	Emission rates of vRES and energy purchased, respectively (tCO$_2$e/MWh)	N_i, N_ς	Number of buses and substations, respectively
g_k, b_k, S_k^{max}	Conductance, susceptance, and flow limit of branch k (Ω, Ω, **MVA**)	V_{nom}	Nominal voltage (kV)
MP_k, MQ_k	Big-M parameters associated with active and reactive power flows through branch k	Z_{ij}, R_k, X_k	Impedances of branch i-j (Ω)
$OC_{g,i,s,h}$	Operation cost of unit energy production by vRES (€/MWh)	$\lambda_{s,h}^{CO_2e}$	Price of emissions (€/tons of CO$_2$ equivalent)
MP_k, MQ_k	Big-M parameters associated with active and reactive power flows through branch k	$\lambda_{s,h}^\varsigma$	Price of electricity purchased upstream (€/MWh)
$OC_{g,i,s,h}$	Operation cost of unit energy production by vRES (€/MWh)	ρ_s, π_w	Probability of hourly scenario s and weight (in hours) of hourly snapshot group h
$v_{s,h}^P, v_{s,h}^Q$	Penalty for active and reactive unserved power, respectively (€/MW, €/MVAr)	$\rho f_{ss}, \rho f_g$	Power factor of substation and DGs, respectively
L	Total number of linear segments	α_l, β_l	Slopes of linear segments
Variables	Definitions	**Variables**	Definitions
$PD_{s,h}^i, QD_{s,h}^i$	Active and reactive power demand at node i (MW, MVAr)	$P_{i,s,h}^{NS}$	Unserved power at node i (MW)
$P_{g,i,s,h}, Q_{g,i,s,h}$	Active and reactive power produced by vRESs (MW)	$Q_{i,s,h}^{NS}$	Unserved power at node i (MW)
$P_{\varsigma,s,h}^{SS}, Q_{\varsigma,s,h}^{SS}$	Active and reactive power imported from the grid (MW)	V_i, V_j	Voltage magnitudes at nodes i and j (kV)
P_k, Q_k, θ_k	Active and reactive power flows, and voltage angle difference of link k (MW, MVAr, radians)	$u_{k,h}$	Utilization variables of existing lines
PL_k, QL_k	Active and reactive power losses (MW, MVAr)	θ_i, θ_j	Voltage angles at node i and j (radians)
$PL_{\varsigma,s,h}, QL_{\varsigma,s,h}$	Active and reactive power losses at substation ς (MW, MVAr)	$\lambda_{s,h}$	Real-time price of electricity (€/MWh)
$p_{k,s,h,l}, q_{k,s,h,l}$	Step variables used in the linearization of quadratic flows (MW, MVAr)		
Functions	Definitions	**Functions**	Definitions
EC_h^{SS}	Expected cost of energy imported through the substation level	EC_h^{vRES}	Expected cost of energy produced by vRES
$EmiC_h^{vRES}$	Expected emission cost due to vRES power production (€)	$EmiC_h^{SS}$	Expected emission cost of energy imported through the substations (€)
TEC	Total expected costs of supplied energy (€)	$TENSC$	Total expected costs of energy not supplied (€)
$TEmiC$	Total expected costs of emissions (€)		

Appendix B

There are a number of ways to linearize the quadratic functions in (14) through (16), such as incremental, multiple choice, convex combination, and other approaches in the literature. However, as mentioned earlier, the quadratic terms are linearized via a piecewise linearization method, which is thoroughly described in [26,27]. For the sake of brevity, here, we only show the piecewise representations of $P_{k,s,h}^2$ and $Q_{k,s,h}^2$. Others follow the same procedure and involve similar sets of constraints.

The approach (which is based on a first-order approximation of the nonlinear curve) uses a sufficiently large number of linear segments, *L*. To this end, two non-negative auxiliary variables are introduced for each of the flows P_k and Q_k such that $P_k = P_k^+ - P_k^-$ and $Q_k = Q_k^+ - Q_k^-$. Note that these auxiliary variables (i.e., P_k^+, P_k^-, Q_k^+, Q_k^-) represent the positive and negative flows of P_k and Q_k, respectively. This helps one to consider only the positive quadrant of the nonlinear curve, resulting in a significant reduction in the mathematical complexity, and by implication the computational burden. In this case, the associated linear constraints are:

$$P_{k,s,h}^2 \approx \sum_{l=1}^{L} \alpha_{k,l} p_{k,s,\,h,l} \tag{B1}$$

$$Q_{k,s,h}^2 \approx \sum_{l=1}^{L} \beta_{k,l} q_{k,s,\,h,l} \tag{B2}$$

$$P_{k,s,h}^+ + P_{k,s,h}^- = \sum_{l=1}^{L} \alpha_{k,l} p_{k,s,\,h,l} \tag{B3}$$

$$Q_{k,s,h}^+ + Q_{k,s,h}^- = \beta_{k,l} q_{k,s,\,h,l} \tag{B4}$$

where $p_{k,s,h,l} \leq P_k^{max}/L$; $q_{k,s,h,l} \leq Q_k^{max}/L$; $\alpha_{k,l} = (2l-1)P_k^{max}/L$; and $\beta_{k,l} = (2l-1)Q_k^{max}/L$.

References

1. Papaefthymiou, G.; Dragoon, K. Towards 100% renewable energy systems: Uncapping power system flexibility. *Energy Policy* **2016**, *92*, 69–82. [CrossRef]
2. International Energy Agency (IEA). *Empowering Variable Renewables—Options for Flexible Electricity Systems*; OECD: Paris, France, 2008.
3. Santos, S.F.; Fitiwi, D.Z.; Cruz, M.R.M.; Cabrita, C.M.P.; Catalão, J.P.S. Impacts of optimal energy storage deployment and network reconfiguration on renewable integration level in distribution systems. *Appl. Energy* **2017**, *185*, 44–55. [CrossRef]
4. Brouwer, A.S.; van den Broek, M.; Seebregts, A.; Faaij, A. Impacts of large-scale Intermittent Renewable Energy Sources on electricity systems, and how these can be modeled. *Renew. Sustain. Energy Rev.* **2014**, *33*, 443–466. [CrossRef]
5. Ceaki, O.; Vatu, R.; Mancasi, M.; Porumb, R.; Seritan, G. Analysis of Electromagnetic Disturbances for Grid-Connected PV Plants. In Proceedings of the 2015 MEPS—International Conference Modern Electric Power Systems, Wroclaw, Poland, 6–9 July 2015.
6. Ceaki, O.; Vatu, R.; Golovanov, N.; Porumb, R.; Seritan, G. Analysis of the grid-connected PV plants behavior with FACTS influence. In Proceedings of the 49th International Universities Power Engineering Conference (UPEC), Cluj-Napoca, Romania, 2–5 September 2014.
7. Panagiotis, K.; Lambros, E. *Electricity Distribution*; Springer: New York, NY, USA, 2016.
8. Hossain, M.S.; Madlool, N.A.; Rahim, N.A.; Selvaraj, J.; Pandey, A.K.; Khan, A.F. Role of smart grid in renewable energy: An overview. *Renew. Sustain. Energy Rev.* **2016**, *60*, 1168–1184. [CrossRef]
9. Schachter, J.A.; Mancarella, P. A critical review of Real Options thinking for valuing investment flexibility in Smart Grids and low carbon energy systems. *Renew. Sustain. Energy Rev.* **2016**, *56*, 261–271. [CrossRef]
10. Yenginer, H.; Cetiz, C.; Dursun, E. A review of energy management systems for smart grids. In Proceedings of the 2015 3rd International Istanbul, Smart Grid Congress and Fair (ICSG), Istanbul, Turkey, 29–30 April 2015; pp. 1–4.
11. Kulkarni, S.N.; Shingare, P. A review on Smart Grid Architecture and Implementation Challenges. In Proceedings of the 2016 International Conference on Electrical, Electronics, and Optimization Techniques (ICEEOT), Chennai, India, 3–5 March 2016.
12. Zhou, X.; Cui, H.; Ma, Y.; Gao, Z. Research review on smart distribution grid. In Proceedings of the 2016 IEEE International Conference on Mechatronics and Automation (ICMA), Harbin, China, 7–10 August 2016; pp. 575–580.

13. Udgave, A.D.; Jadhav, H.T. A review on Distribution Network protection with penetration of Distributed Generation. In Proceedings of the 2015 IEEE 9th International Conference on Intelligent Systems and Control (ISCO), Coimbatore, India, 9–10 January 2015; pp. 1–4.

14. Bhimarasetti, R.T.; Kumar, A. A New Contribution to Distribution Load Flow Analysis for Radial and Mesh Distribution Systems. In Proceedings of the 2014 International Conference on Computational Intelligence and Communication Networks, Bhopal, India, 14–16 November 2014; pp. 1229–1236.

15. Arritt, R.F.; Dugan, R.C. Review of the Impacts of Distributed Generation on Distribution Protection. In Proceedings of the 2015 IEEE Rural Electric Power Conference, Asheville, NC, USA, 19–21 April 2015; pp. 69–74.

16. Tiwari, A.K.; Mohanty, S.R.; Singh, R.K. Review on protection issues with penetration of distributed generation in distribution system. In Proceedings of the 2014 International Electrical Engineering Congress (iEECON), Chonburi, Thailand, 19–21 March 2014; pp. 1–4.

17. Celli, G.; Pilo, F.; Pisano, G.; Cicoria, R.; Iaria, A. Meshed vs. radial MV distribution network in presence of large amount of DG. In Proceedings of the IEEE PES Power Systems Conference and Exposition, New York, NY, USA, 10–13 October 2004; pp. 1357–1362.

18. Yu, P.; Venkatesh, B.; Yazdani, A.; Singh, B.N. Optimal Location and Sizing of Fault Current Limiters in Mesh Networks Using Iterative Mixed Integer Nonlinear Programming. *IEEE Trans. Power Syst.* **2016**, *31*, 4776–4783. [CrossRef]

19. Zubo, R.H.A.; Mokryani, G.; Rajamani, H.-S.; Aghaei, J.; Niknam, T.; Pillai, P. Operation and planning of distribution networks with integration of renewable distributed generators considering uncertainties: A review. *Renew. Sustain. Energy Rev.* **2017**, *72*, 1177–1198. [CrossRef]

20. Alvarez-Herault, M.-C.; N'Doye, N.; Gandioli, C.; Hadjsaid, N.; Tixador, P. Meshed distribution network vs reinforcement to increase the distributed generation connection. *Sustain. Energy Grids Netw.* **2015**, *1*, 20–27. [CrossRef]

21. Davoudi, M.; Cecchi, V.; Agüero, J.R. Increasing penetration of distributed generation with meshed operation of distribution systems. In Proceedings of the North American Power Symposium (NAPS), Pullman, WA, USA, 7–9 September 2014; pp. 1–6.

22. Chalapathi, B.; Agrawal, D.; Murty, V.; Kumar, A. Optimal placement of Distribution Generation in weakly meshed Distribution Network for energy efficient operation. In Proceedings of the 2015 Conference on Power, Control, Communication and Computational Technologies for Sustainable Growth (PCCCTSG), Kurnool, India, 11–12 December 2015; pp. 150–155.

23. Ivic, D.; Macanovic, D.; Sosic, D.; Stefanov, P. Weakly meshed distribution networks with distributed generation—Power flow analysis using improved impedance matrix based algorithm. In Proceedings of the International Symposium on Industrial Electronics (INDEL), Banja Luka, Bosnia Herzegovina, 3–5 November 2016; pp. 1–6.

24. Yang, H.; Bae, T.; Kim, J.; Kim, Y.H. Load model technique for mesh-structured power distribution network. In Proceedings of the 2012 4th Asia Symposium on Quality Electronic Design (ASQED), Penang, Malaysia, 10–11 July 2012; pp. 219–222.

25. Yu, L.; Czarkowski, D.; de León, F.; Bury, W. A time sequence load-flow method for steady-state analysis in heavily meshed distribution network with DG. In Proceedings of the 2013 8th International Conference on Compatibility and Power Electronics (CPE), Ljubljana, Slovenia, 5–7 June 2013; pp. 25–30.

26. Fitiwi, D.Z.; Olmos, L.; Rivier, M.; de Cuadra, F.; Pérez-Arriaga, I.J. Finding a representative network losses model for large-scale transmission expansion planning with renewable energy sources. *Energy* **2016**, *101*, 343–358. [CrossRef]

27. Zhang, H.; Heydt, G.T.; Vittal, V.; Quintero, J. An Improved Network Model for Transmission Expansion Planning Considering Reactive Power and Network Losses. *IEEE Trans. Power Syst.* **2013**, *28*, 3471–3479. [CrossRef]